DROP EVAPORATION ON AN ISOTHERMAL OR ADIABATIC SOLID SURFACE

M. Ait Saada[1], S. Chikh[1], L. Tadrist[2], S. Radev[3]
[1] USTHB – Faculty of Mechanical and Process Engineering (FGMGP)
Laboratory of Multiphase Transport and Porous Media (LTPMP)
B.P.32, El Alia, Bab Ezzouar 16111 Alger, Algeria
[2] Aix-Marseille Université, Polytech'Marseille, Laboratoire IUSTI, CNRS UMR 7343,
Technopôle de Château Gombert, 5 rue Enrico Fermi, 13453 Marseille, France
[3] Institute of Mechanics, Bulg. Acad. Sci., 4,acad. G. Bonchev str., 1113 Sofia, Bulgaria

Abstract

A quasi-steady state diffusion model is developed to simulate numerically the evaporation of a pinned or depinned sessile drop of water. A numerical approach based on the finite volume method is adopted to assess heat and mass transfer rates. The results show that the overall heat and mass transfer rates at the liquid-gas interface change from the case where the drop is supplied with heat from the substrate with a very high thermal conductivity to the case where the drop on a substrate of very low thermal conductivity receives the needed energy mainly from the gas phase. The drop is cooled under the evaporation effect and its mean temperature decreases considerably and achieves 16°C on an ideal thermal insulator.

Key words: Evaporation, Sessile drop, Heat and mass transfer, Interface, Diffusion

1. Introduction

Coupled heat and mass transfer during evaporation of a sessile drop on a substrate is a complex phenomenon although it seems simple. Indeed, the presence of three phases, solid, liquid and gas, adds in complexity particularly at both solid-liquid and liquid-gas interfaces. The kinetics of evaporation and the dynamics of the contact line are not perfectly understood and research developments are still needed to clarify many related points. Many authors investigated the evaporation of a sessile drop which usually occurs under constant wetting radius and variable contact angle or inversely [1, 2]. Thermal properties or heating temperature of substrate were shown to have an effect on the evaporation process of a sessile drop [3-5]. David et al. [3] showed that the evaporating water sessile drop induced an important cooling effect when the substrate was thermally insulating. Experimental data under a reduced pressure environment showed that the effect of substrate thermal conductivity became important as evaporation was increased. Dunn et al. [4] reported experimental results on the strong influence of the thermal conductivity of the substrate and developed a model including the variation of the saturation concentration with temperature at the free surface of the pinned sessile drop. Ait saada et al. [5] developed a convection-diffusion model to analyze the effect of buoyant convection in the surrounding air. Their predictions showed that the diffusion model underestimated the overall evaporation rate by 8.5% for a wall temperature equal to an ambient temperature of 25 °C and by 27.3% for a wall temperature of 70 °C in comparison to that obtained with a convection-diffusion model.

In this study, a numerical analysis is carried out using a diffusion model to work out the problem of evaporation of a small water drop on a substrate which can be a perfect thermal insulating or a perfect heat conductor. Hence, the substrate is assimilated to an adiabatic or isothermal solid surface. The model proposed accounts for heat conduction in both liquid and gas phases and for water vapour diffusion in the surrounding air. The computer program is implemented to couple between the drop and the surrounding air. The temperature and concentration profiles are first determined and then the local heat flux is computed at the liquid-gas interface. The mass transfer is quantified locally by the mass flux and globally by the evaporation rate on the drop surface. The evaporation of a drop on a perfect thermal insulating substrate is compared to that of a drop on a perfect thermal conductor substrate.

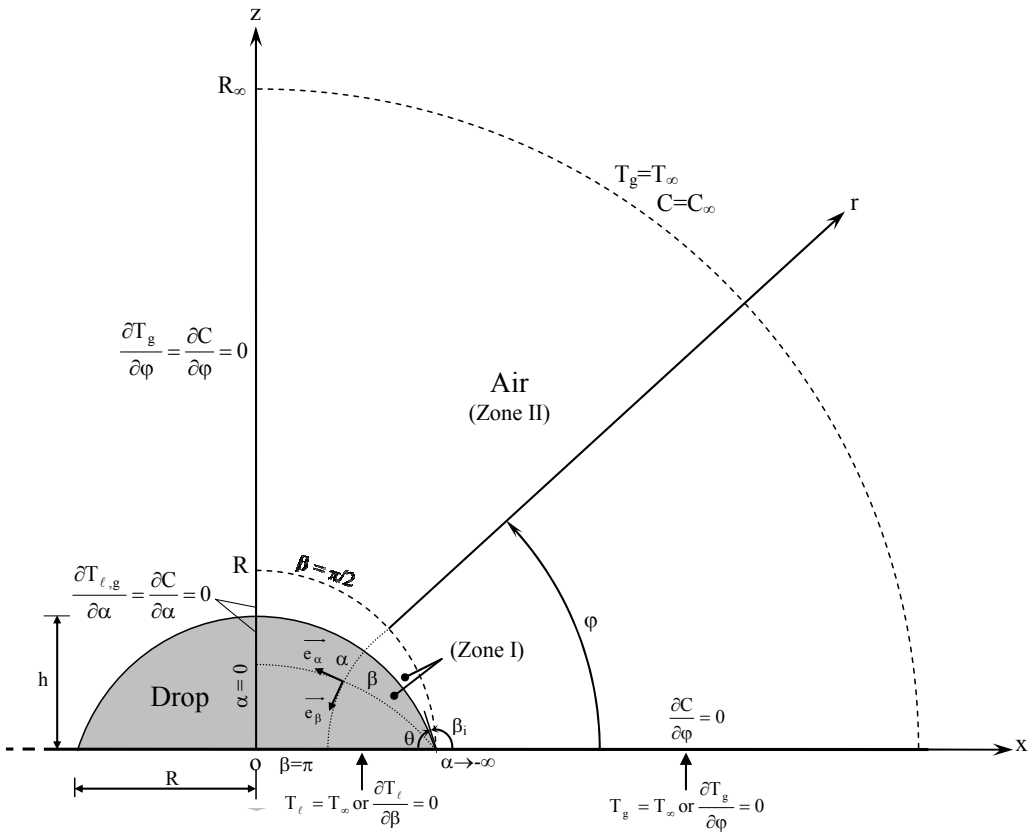

Figure 1: Water drop of spherical cap shape deposited on a horizontal substrate.

2. Mathematical Formulation

A 10 mm^3 droplet of pure water is deposited on a non heating horizontal solid surface, as shown in figure 1. The evaporation of the drop occurs in surrounding moist air at room temperature T_∞ of 25°C and relative humidity H_a of 40%. The drop has a shape of a spherical cap controlled by surface tension effect because its size is lower than the capillary length.

In our investigation, the evaporation occurs either in pinned mode where the contact radius R is kept constant and the contact angle θ variable in time or in de-pinned mode where inversely R is variable and θ constant in time. The diffusion model is considered in the present study and for instance convective flow inside or outside the drop is neglected. Hence, heat transfer in the liquid or gas phase is assumed to occur by conduction mode alone. The saturated vapor resulting from phase change at the liquid-gas interface is transferred by diffusion to ambient moist air. Mass transfer in the surrounding gas and heat transfer in the two phases are assumed to evolve symmetrically around the vertical axis (oz) and evaporation takes place in a quasi steady state because of the slow evaporation process inducing a slow motion of the liquid–gas interface.

The mathematical formulation of the considered problem is based on the conservative energy equation in the phases and the concentration equation in the gas phase. The dimensionless governing equations are written in toroidal coordinates (α, β) in zone (I) and in spherical coordinates (r, φ) in zone (II), see Fig. 1. The toroidal coordinate system allows better handling and localizing the moving liquid-air interface ($\beta=\beta_i$).

i) in the liquid phase of zone (I),

$$\frac{\partial}{\partial\alpha}\left(H\,H_\phi\,\frac{\partial T_\ell^*}{H\partial\alpha}\right)+\frac{\partial}{\partial\beta}\left(H\,H_\phi\,\frac{\partial T_\ell^*}{H\partial\beta}\right)=0 \qquad (1)$$

ii) in the gas phase of zone (I),

$$\frac{\partial}{\partial\alpha}\left(H\,H_\phi \frac{\partial T_g^*}{H\partial\alpha}\right)+\frac{\partial}{\partial\beta}\left(H\,H_\phi \frac{\partial T_g^*}{H\partial\beta}\right)=0 \tag{2 a}$$

$$\frac{\partial}{\partial\alpha}\left(H\,H_\phi \frac{\partial C^*}{H\partial\alpha}\right)+\frac{\partial}{\partial\beta}\left(H\,H_\phi \frac{\partial C^*}{H\partial\beta}\right)=0 \tag{2 b}$$

iii) in zone (II),

$$\frac{\partial}{\partial r^*}\left(r^{*2}\cos(\varphi)\frac{\partial T_g^*}{\partial r^*}\right)+\frac{\partial}{\partial\varphi}\left(r^*\cos(\varphi)\frac{\partial T_g^*}{r^*\partial\varphi}\right)=0 \tag{3 a}$$

$$\frac{\partial}{\partial r^*}\left(r^{*2}\cos(\varphi)\frac{\partial C^*}{\partial r^*}\right)+\frac{\partial}{\partial\varphi}\left(r^*\cos(\varphi)\frac{\partial C^*}{r^*\partial\varphi}\right)=0 \tag{3 b}$$

The reduced variables are scaled with respect to the initial contact radius R_0 for length variables, the dimensionless temperature is given by $T^* = T/T_\infty$ and the dimensionless concentration $C^* = (C - C_\infty)/\Delta C$ where $C_\infty = H_a C_v(T_\infty)$, $\Delta C = (1 - H_a) C_v(T_\infty)$, $C_v(T_\infty)$ being the saturation concentration at T_∞. The dimensionless metric coefficients of the toroïdal coordinate system are defined by:

$$H = H_\alpha = H_\beta = \frac{1}{\cosh\alpha - \cos\beta},\quad H_\phi = -H\sinh\alpha \tag{4}$$

Boundary conditions associated with the governing equations are indicated in figure 1 where the solid surface is considered adiabatic or maintained isothermal at the ambient temperature. Conditions of no temperature or concentration jump as well as conditions of heat or mass flux continuity are applied at the interface between zones (I) and (II).

$$T_g^{*I} = T_g^{*II}\ ,\quad \left(\frac{\partial T_g^*}{H\partial\beta}\right)^I_{\pi/2} = -\left(\frac{\partial T_g^*}{\partial r'^*}\right)^{II}_1 \quad\text{and}\quad \left(\frac{\partial C^*}{H\partial\beta}\right)^I_{\pi/2} = -\left(\frac{\partial C^*}{\partial r'^*}\right)^{II}_1 \tag{5}$$

In addition, no temperature jump condition is applied at the surface of the drop where air is in a saturated state; its vapor concentration depends on temperature according to a polynomial relationship:

$$C_v(T) = \sum_{i=0}^{4} a_i T^i \tag{6 a}$$

The coefficients a_0, a_1, a_2, a_3 and a_4 are chosen to fit experimental data of Raznjevic [6]. Moreover, the dimensionless mass flux of evaporation from the drop, noted J^*, must satisfy the local energy balance, expressed by:

$$\left(\frac{\Delta C}{\rho_g}\right)\frac{Ja}{Le}J^* - Rk_g^{-1}\left.\frac{\partial T_\ell^*}{H\partial\beta}\right|_{\beta_i} + \left.\frac{\partial T_g^*}{H\partial\beta}\right|_{\beta_i} = 0 \tag{6 b}$$

$Ja = h_{\ell g}/(c_{pg}T_\infty)$ is the Jacob number where h_{lg} is the latent heat of evaporation and $Le = (\alpha_T/D)_g$ is the Lewis number.

The local heat flux is evaluated at the drop surface in each side in order to quantify the contribution of each phase to the evaporation process. The heat exchanges with the liquid phase, Q_l, or gas phase, Q_g, over the whole drop surface are obtained by:

$$Q_\ell^* = \frac{Q_\ell}{2\pi R_0 k_\ell T_\infty} = \int_0^{-\infty}\left.\frac{\partial T_\ell^*}{H\partial\beta}\right|_{\beta_i} H_\phi H d\alpha \tag{7 a}$$

$$Q_g^* = \frac{Q_g}{2\pi R_0 k_\ell T_\infty} = Rk_g\int_0^{-\infty}\left.\frac{\partial T_g^*}{H\partial\beta}\right|_{\beta_i} H_\phi H d\alpha \tag{7 b}$$

The local mass flux J on the drop surface is related to the concentration gradient. In a dimensionless form, it is expressed as:

$$J^* = \frac{J}{D\dfrac{\Delta C}{R_0}} = \left.\frac{\partial C^*}{H\partial\beta}\right|_{\beta_i} \tag{8 a}$$

The evaporation rate $\dot{M}$ over the whole interface is determined by the following equation:

$$\dot{M}^* = \frac{\dot{M}}{2\pi R_0 D \Delta C} = \int_0^{-\infty} \left.\frac{\partial C^*}{H\partial\beta}\right|_{\beta_i} H_\phi H d\alpha \tag{8 b}$$

3. Numerical procedure and validation

The set of governing partial differential equations (1) to (3) with the corresponding boundary and interface conditions are discretized by the use of the control volume method [7]. A zonal grid is applied in the corresponding coordinate system within each zone. A second order central differencing scheme (CDS) which is sufficiently accurate for a diffusion transport phenomena is implemented. The set of obtained algebraic equations are solved using a combination of the tridiagonal matrix algorithm TDMA and the Gauss-Seidel iterative method. The temperature and concentration solution reach satisfactory convergence during the iterative process once the maximum relative error on the dependent variable (T^*, C^*) is lower than 0.1% and the maximum allowable absolute residue in the conservative equations is less than 10^{-5}.

A validation of the computer program is carried out by comparing the numerical results with the experimental ones of Hu and Larson [1] and Song et al. [2]. Figure 2 presents the evolution of the drop volume during evaporation on a glass slide. An excellent agreement is found with the experimental results of these authors when a diffusion model is used and the substrate is considered in isothermal condition at 25°C; a maximum deviation less than 5% is obtained.

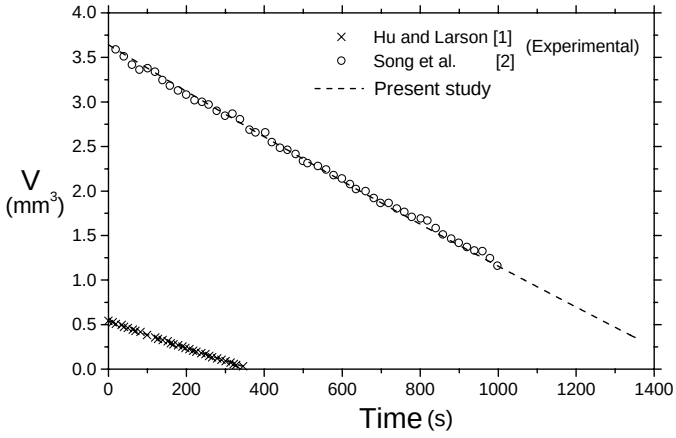

Figure 2: Drop volume variation with time predicted using the developed numerical simulation. The results are compared with experimental results of Hu and Larson (V_0 = 0.54 mm^3, θ_0 = 42°, D = 26.1×10^{-6} m^2/s, H_a = 40%) and Song et al. (V_0 = 3.64 mm^3, θ_0 = 57.2°, D = 25×10^{-6} m^2/s, H_a = 40%).

4. Results and discussion

Results are presented in this section for a water drop of 10 mm^3 with an initial contact radius of 1.86 mm, placed on an adiabatic or isothermal solid surface covered by a very thin layer of aluminum imposing an initial contact angle of 78°. Figure 3 presents temperature and concentration fields. The isotherms distribution exhibits closed contour curves in the region of the liquid-gas interface corresponding to a cooled zone resulting from the phase change accompanied by a decrease in temperature below 25°C. So there is a cooling effect in the drop and its vicinity. For the adiabatic case, the temperature is variable in the environment gas while it is almost constant in the droplet. In this case the needed energy for evaporation comes only from the surrounding air. The saturation concentration is constant and the water vapor diffuses almost uniformly to the atmosphere along the drop surface due to the shape of the drop close to a hemisphere (θ = 78 °). For the isothermal case, the

temperature increases in liquid and gas phases, resulting in a reduction of the extent of the cold zone. The minimum temperature located at the top of the drop is raised and temperature gradients in the liquid phase increase while they decrease in the gas phase. Concentration gradients are high close to the liquid-gas interface and take the highest value at the contact line where most of the evaporation occurs.

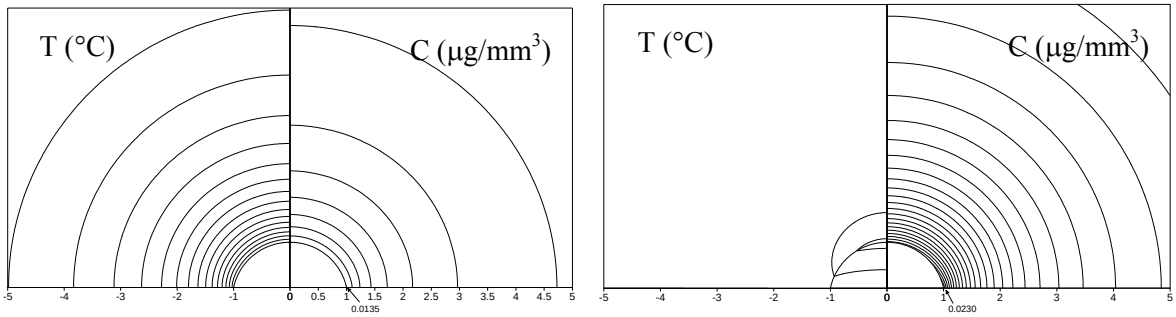

(a) Adiabatic case ($k_s = 0$) (b) Isothermal case ($k_s \rightarrow \infty$)

Figure 3: Isotherms and iso-concentrations distribution at the beginning of evaporation (ΔT=0.25°C, ΔC=0.0005 μg/mm^3).

The thermal state of the drop is indicated by the temperature distribution plotted along the solid-fluid interface and the drop surface as shown in Fig. 4. The temperature is initially at 25°C everywhere, so with no heating and with an isothermal solid surface, the temperature along the drop surface increases from the apex to the contact line where it undergoes a strong variation. The maximum temperature difference ΔT_{max} within the drop, located on the symmetry axis at r/R=0, is about 1°C. For an adiabatic solid surface, a better cooling effect is obtained and the temperature goes down to 16°C with nearly uniform temperature in the liquid phase. Then, it looks like an isothermal drop on an adiabatic wall. The temperature at the drop base is nearly constant and starts increasing on the dry side of solid surface to reach 25°C at a distance which represents the boundary of the cold zone resulting from evaporation.

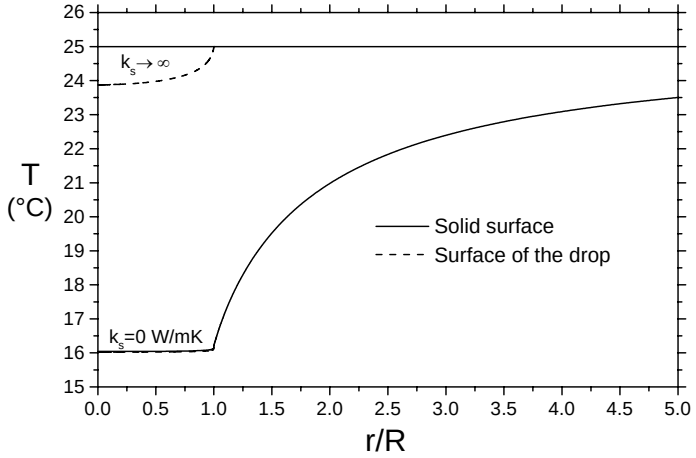

Figure 4: Temperature distribution on the solid surface and on the drop surface at the beginning of evaporation.

Figure 5 displays the evaporation mass flux distribution which is uniform all along the drop surface until it approaches the contact line where it strongly increases. This behavior is similar for the two cases of solid surface, but the increase towards the contact line is much less pronounced for the ideal adiabatic substrate. In the latter case the heat supply to the drop surface comes from the surrounding air inducing the lowest temperature of the drop and consequently the lowest mass flux. But this is true at the beginning of evaporation where the contact angle is of a high value (78°). The strong variation of the mass exchanges close to the contact line is independent of the nature of the solid surface when the contact angle is small.

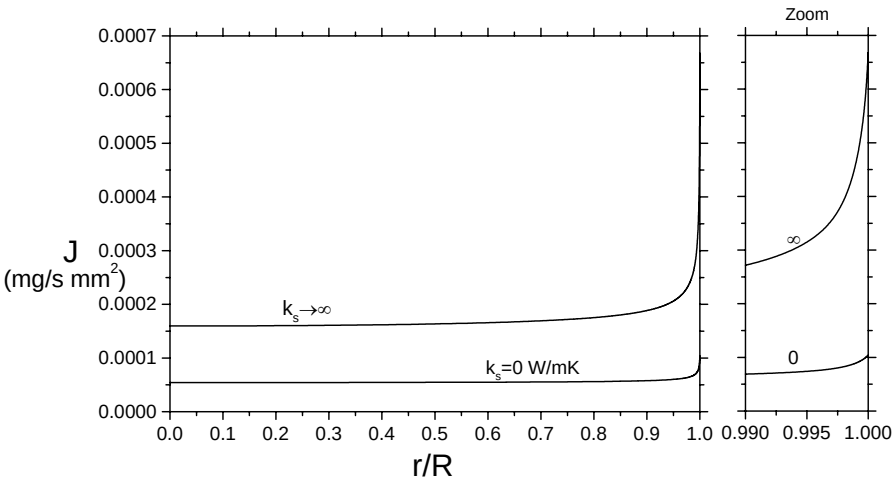

Figure 5: Local evaporation flux on the drop surface at the beginning of evaporation.

Figure 6 shows the heat transfer rate from both the liquid and gas sides. Heat transfer rate reduces during the evaporation process. This is mainly due to the drop surface that decreases. In terms of heat supply, it is clear that when the substrate is a good heat conductor, the heat input to the interface comes mainly from the liquid phase, but it stiffly decreases with time in de-pinned evaporation mode. The reason may be the base surface area that shrinks rapidly and then less energy is taken from the substrate. However, for the ideal adiabatic substrate (k_s=0), heat is supplied from the surrounding air and then the behavior is similar in the two evaporation modes pinned or de-pinned.

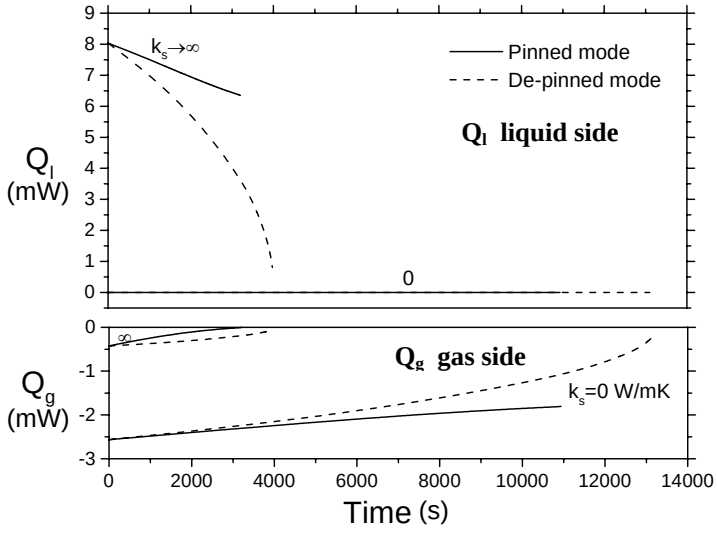

Figure 6: Evolution of heat amount exchanged at the drop surface for the pinned or de-pinned evaporation mode.

Mass transfer results are displayed in Fig. 7. The time evolution of the evaporation rate shows a continuous decrease with stiff slope in the de-pinned evaporation mode particularly at high thermal conductivity of the substrate. This means that the evaporation kinetics is faster for a de-pinned drop than a pinned one. The evaporation rate of a pinned drop is higher and undergoes a linear decrease in time.

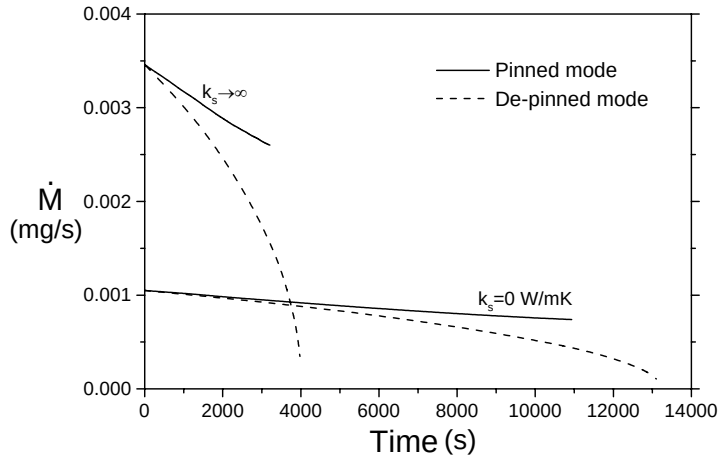

Figure 7: Evolution of the evaporation rate for the pinned or de-pinned evaporation mode.

5. Conclusion

A quasi steady state diffusion model is considered which combines the heat equation in both liquid and gas phases and the mass diffusion equation in the surrounding air. Coupling between heat and mass transfer is achieved by accounting for temperature dependency of the saturation concentration at the drop surface and the heat balance at the interface. The numerical results showed that the evaporation rate and the overall heat transfer rate associated with phase change take values which differ from the case of evaporation on an ideal heat conductor ($k_s \to \infty$) with that of evaporation on ideal thermally insulating substrate ($k_s=0$). The evaporation rate is smaller the sessile drop receives energy mainly from the surrounding air. Moreover, a comparison between a pinned and depinned drop shows a faster kinetics of evaporation for a depinned drop.

Acknowledgements: One of the authors (S. Radev) expresses his gratitude to the Bulgarian Scientific Fund for the support in the frame of Project DO 02-75/2008.

References

[1] Song H., Lee Y., Jin S., Kim H.Y. and Yoo J.Y., Prediction of sessile drop evaporation considering surface wettability, *Microelectronic Engineering*, *88, 2011*, *Pages 3249-3255.*

[2] Hu H. and Larson R.G. (2002) Evaportion on a sessile droplet on a substrate, J.Phys.Chem.B, Vol.106, pp. 13334-1344.

[3] David S., Sefiane K. and Tadrist L., Experimental investigation of the effect of thermal properties of the substrate in the wetting and evaporating of sessile drops, *Colloids and surfaces A: Physicochemical and Engineering Aspects,* 2007, 298, pp. 108-114.

[4] Dunn G.J., Wilson S.K., Duffy B.R., David S. and Sefiane K., The strong influence of substrate conductivity on droplet evaporation, *J. Fluid Mech.*, 2009, 623, pp. 329-351.

[5] Ait Saada M., Chikh S. and Tadrist L., Numerical investigation of heat and mass transfer of an evaporating sessile drop on a horizontal surface, *Phys. Fluids* **22**, 1121.

[6] Raznjevic K., Handbook of thermodynamic tables, Begell House, 1995.

[7] Patankar, S.V., Numerical heat transfer and fluid flow, McGrawHill, Hemisphere, Washington, D.C, 1980.